Supplemental Figure 1: Differentiation state of CMT-luc and LLC-luc cells.

(A) Light microscope images of CMT-luc and LLC-luc cells *in vitro*. (B) qRT-PCR of E-cadherin and Vimentin in CMT-luc and LLC-luc cells in vitro. (C) Log2 transformation of E-cadherin/vimentin ration for CMT-luc and LLC-luc cells as measure by qRT-PCR.

Supplemental Figure 2: Intratumoral myeloid cell populations do not change with PPARγ knockout or activation. WT or PPARγ-MKO mice were injected with CMT-luc cells. Tumor bearing lungs were harvested 21 days post injection. Myeloid cell populations were identified using the markers described. (A) Schematic of the flow cytometry gating strategy used to define tumor myeloid cell populations. After gating on cells using forward and side scatter plots, live cells were selected based on exclusion of DAPI staining. Within the live cell population, neutrophils (Neu) were identified based on positive expression of CD11b and Ly6G. The non-neutrophil (Non-Neu) population of cells that were not double positive for CD11b and Ly6G were then selected. In the non-Neu population, alveolar macrophages (Mac A) were identified based on positive expression of SigF and CD11c. The SigF negative population was then gated on and recruited macrophages (Mac B) were identified based on positive expression of CD11b and CD64. (B) Myeloid cell populations identified across the different groups of mice as percentage of the total live cell population. Tumor myeloid cell populations are compared to those found in normal, uninjected mouse lung (*$p<0.05$, **$p<0.01$ for all tumor groups compared to normal lung). (C) TGF-β1 released from RAW 264.7 macrophages treated with media from CMT cells or media plated in the absence of cells and treated with DMSO or with Pio (10μM). Values were normalized to total RAW 264.7 protein concentration (*$p<0.05$, **$p<0.01$, ***$p<0.001$).

Supplemental Figure 3: TGFβRII knockdown CMT-luc cells are less responsive to TGF-β1 treatment.

(A) Western blot of p-SMAD2, total SMAD2/3 and β-Actin expression in CMT parentals, CMT control shRNA or CMT TGFβRII shRNA (531 and 602) cells treated with TGFβ1. (B) Light microscope images of CMT control shRNA or CMT TGFβRII shRNA (531 and 602) treated with vehicle control or treated with TGFβ1 for 72 hours.

Supplemental Figure 4: Loss of PPARγ in myeloid cells does not affect LLC-luc tumor progression.

PPARγ-WT or PPARγ-MKO mice were orthotopically injected with LLC-luc cells. Tumor bearing lungs were collected 2.5 weeks later, formalin fixed, and paraffin embedded. (A) Primary tumor size was measured by caliper and reported as the tumor volume in mm^3. (B) Number of secondary lung metastases was counted on H&E stained sections of the lungs. (C) Incidence of metastasis reported as the percent of mice with metastasis to the other lobes of the lung (secondary lung), liver, or brain as measured by bioluminescence.

Supplemental Figure 5: LLC cell response to TGF-β1 treatment.

(A) Proliferation of LLC-luc cells treated with TGF-β1 or vehicle control *in vitro*, measured as change in total luminescence (*$p<0.05$ for TGF-β1 treated compared to respective vehicle treated controls). (B) Number of migrating cells in transwell migration assays using LLC-luc cells treated with TGF-β1 or vehicle control (**$p<0.01$, ***$p<0.001$). (C) qRT-PCR for Zeb1, and Vimentin in LLC-luc cells post TGF-β1 treatment combined with the TGFβRI inhibitor SB431542 or vehicle control (DMSO).

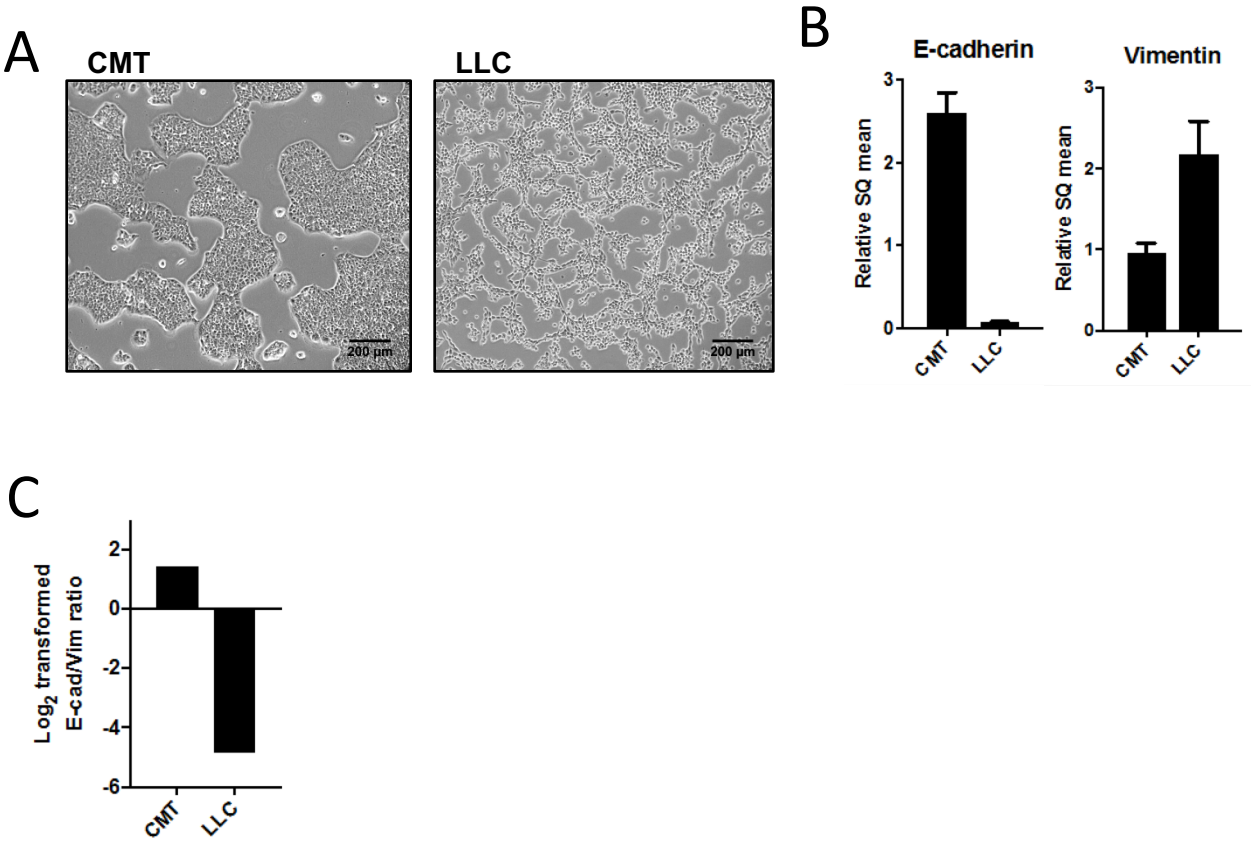

Supplemental Figure 1

Supplemental Figure 2

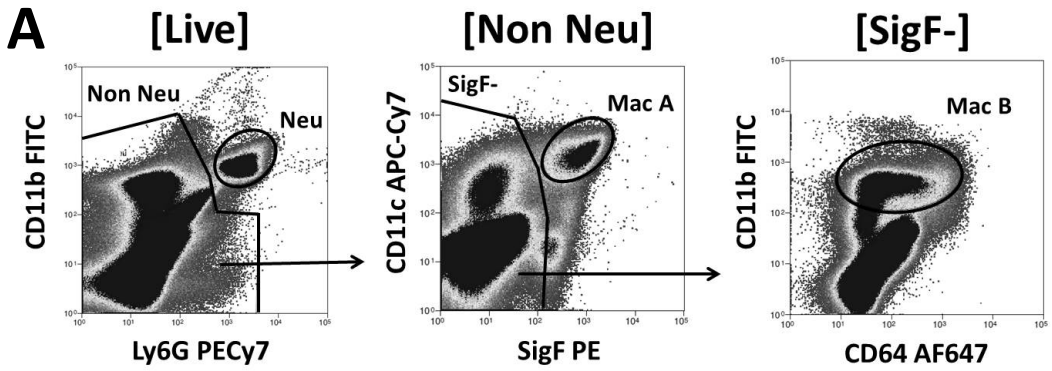

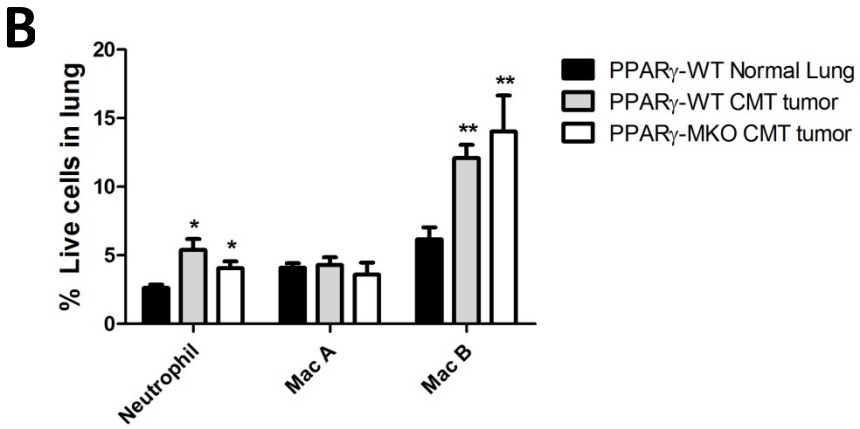

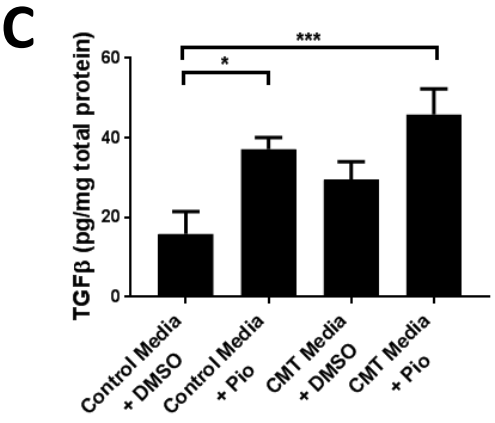

Supplemental Fig. 2

A

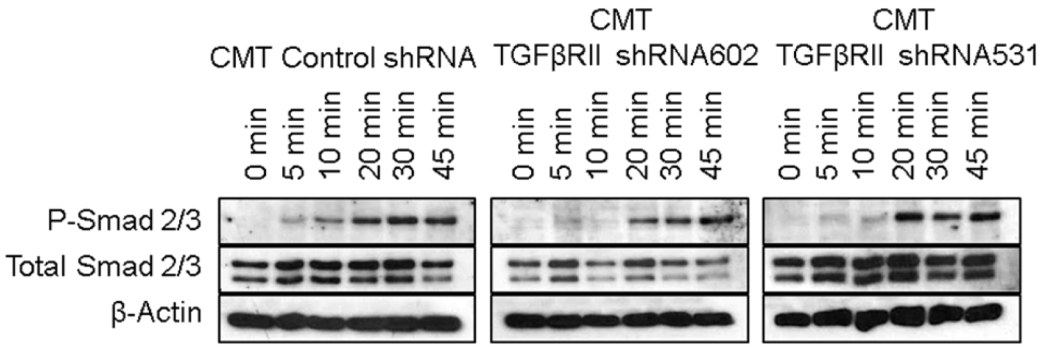

B

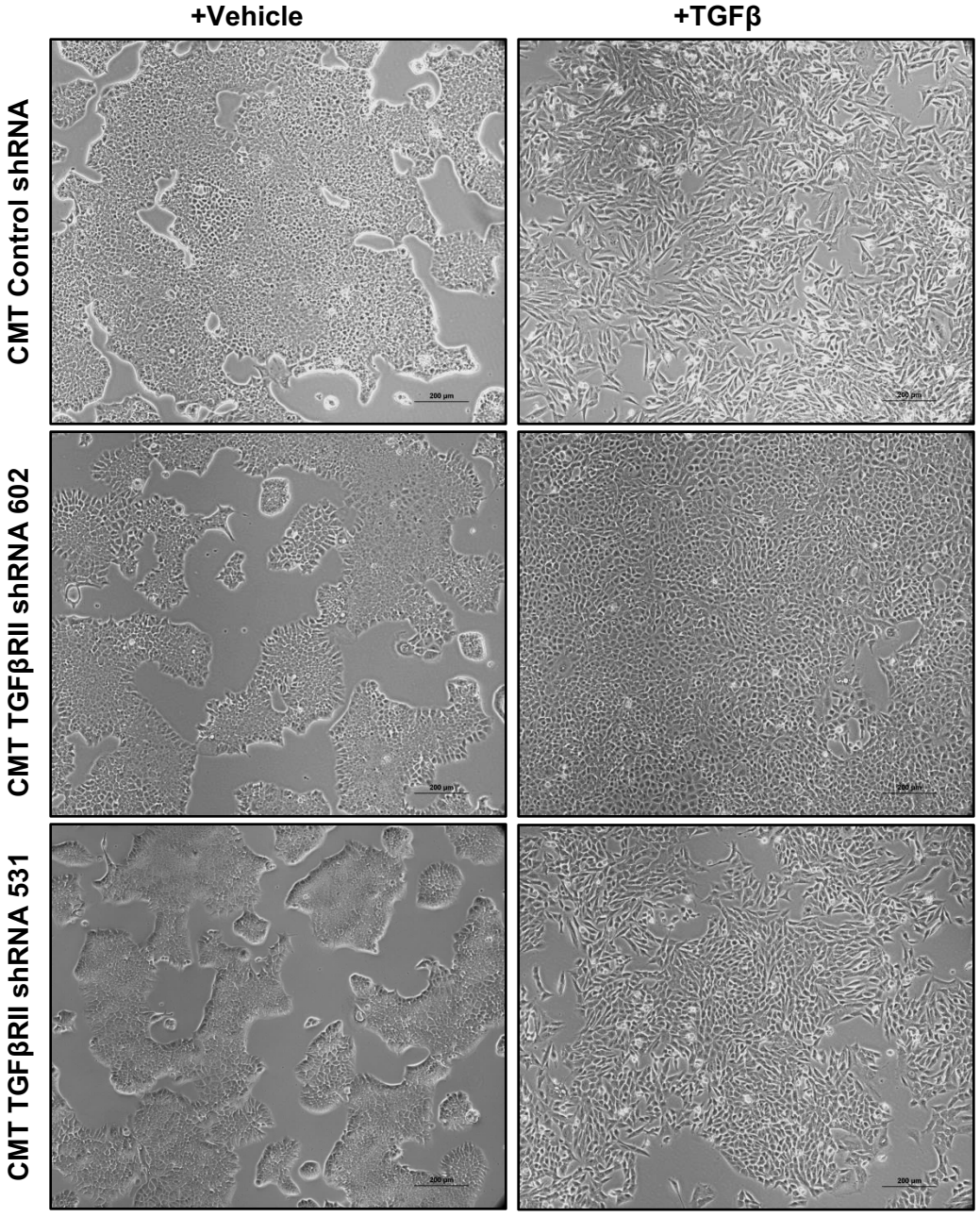

Supplemental Fig. 3

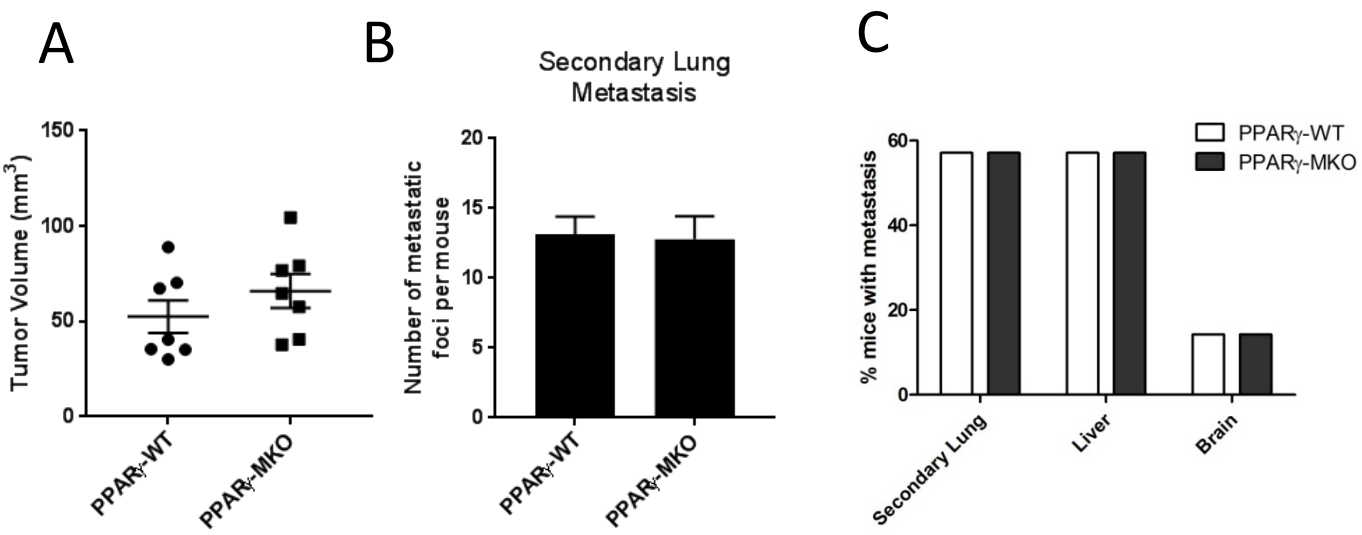

Supplemental Fig. 4

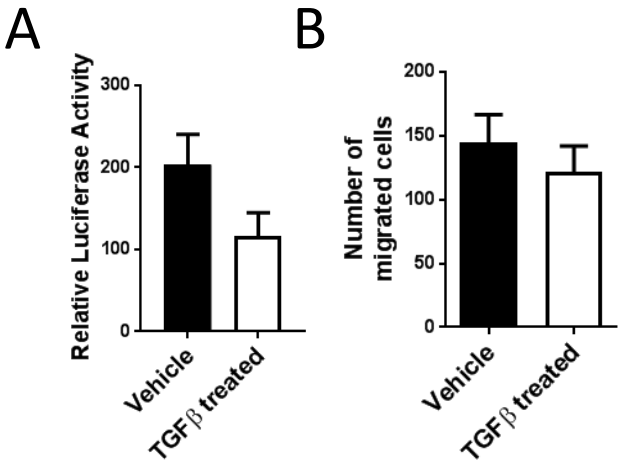

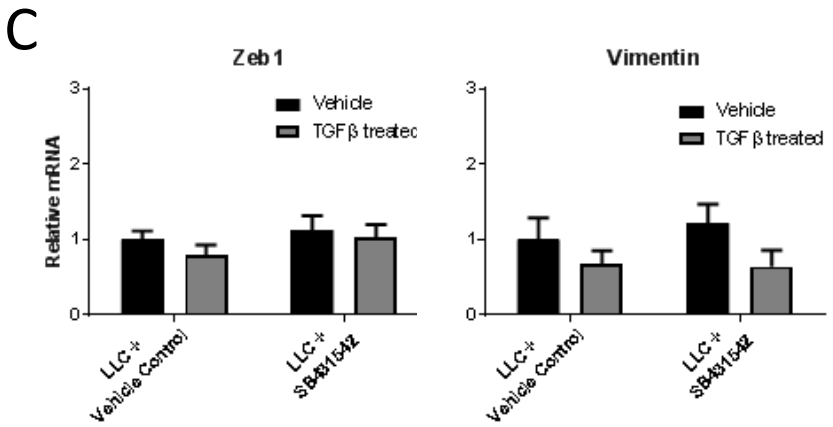

Supplemental Fig. 5